Atmospheric Electricity

https://www.iamas.org/icae/
NEWSLETTER
Vol.33 NO.1 May 2022

INTERNATIONAL COMMISSION ON ATMOSPHERIC ELECTRICITY
IAMAS IUGG

ICAE

ICLP 2022, 2-7 October 2022, South Afirca

ICLP 2022, the 36th International Conference on Lightning Protection, continues the tradition of the preceding 35 conferences by offering a platform for the exchange of scientific and technical information related to lightning phenomena and protection against these phenomena. Hosted by the University of the Witwatersrand (Johannesburg), the conference will be held in 2-7 October 2022 in beautiful Cape Town. Please visit https://iclp2022.org/ for more details.

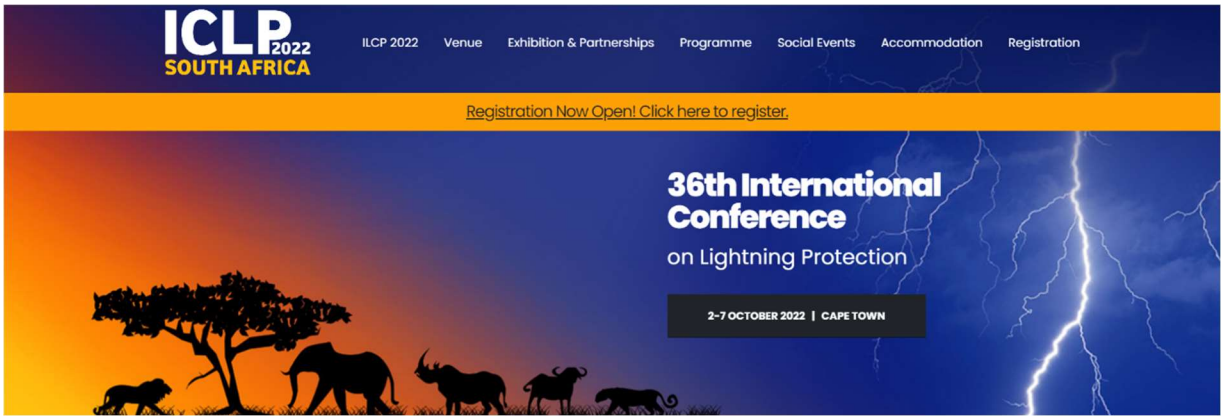

APEMC 2022, 10-13 July 2022, Beijing

The 13th Asia-Pacific International Symposium on Electromagnetic Compatibility & Technical Exhibition (APEMC 2022) will be co-located with and held during the 2022 Beijing EMC Week, Beijing, China, from 10 to 13 July 2022. The Symposium will continue the APEMC spirit to engage and address the world-wide EMC community with a primary focus on the Asia-Pacific region. Please visit the website at https://apemc.org/call-for-papers/.

New website for ICAE

The formal website for ICAE has been moved to https://www.iamas.org/icae/. The old site will no longer be updated.

African Centres for Lightning and Electromagnetics (ACLENet)

ACLENet is pleased to announce the signing of a Memo of Understanding with the Ministry of Disaster Preparedness (MoDPR) in the Office of the Prime Minister of the Government of Uganda that will be the basis for a partnership focusing on disaster mitigation and preparedness as they relate to lightning. Protecting schools, through donor funding and grants has been one of ACLENet's main areas of work. Public safety education, through mass media, is another. Additionally, we will be working to transfer know-how of lightning safety across Africa, one country and one project at a time. The Honorable Minister Hilary Onek (Figure 1) has been a strong proponent of ACLENet's work.

Figure 1. Thumbs up for our work from the Honorable Minister Hilary Onek, Minister of Disaster Preparedness and Member of Parliament, Uganda, as he hosted the commissioning of ACLENet's lightning protection installation at Palabek Secondary School in 2020. To the left is Head Teacher, Mr. Olaa Peter, in blue and Head of the school's Board of Directors in orange.

ACLENet is currently finishing the installation of lightning protection system at Mongoyo Primary School where three children were killed and dozens hospitalized for a single lightning strike to the school in October 2018 (Figure 2). Not only does ACLENet protect schools and do public education, we investigate these mass casualty incidents (MCI) as they

occur to learn more about what can be done to decrease injuries in these events.

A paper that was catalyzed by questions from this investigation and through work with ACLENet's Research Advisory Board was published at ICLP-SIPDA2021 (C.J. Andrews).

ACLENet is happy to be a co-sponsor of ICLP2022, the first ICLP to be held on the continent of Africa. More information and newsletters (published in four languages) on ACLENet's activities can be found at their website.

Figure 2. Isaac Tumuhimbise, Chief Installer for ACLENet, checks materials before Phase 2 installation of lightning protection at Mongoyo Primary School in Uganda, the seventh school that ACLENet has protected. PolyTech, a large lightning protection company in Denmark, donated the materials and funding to protect this school and Engineers Without Borders has been instrumental in facilitating the project.

*I*nstitute of Earth Physics and Space Science (ELKH EPSS), Sopron, Hungary

Contributors from the institute: Karolina Szabóné André, Veronika Barta, Tamás Bozóki, József Bór, Attila Buzás, Ernő Prácser, Gabriella Sátori

In Bór et al., 2022 integrated conductivity of the Earth's crust in the Mátra hills, Hungary was determined by quantifying the frequency-dependent attenuation of the ELF transients under the ground using a new method, i.e., via comparison of lightning-induced ELF transient signals which were detected both in the Mátra Hills and at the reference ELF stations: in the

Széchenyi István Geophysical Observatory (SZIGO, IAGA code: NCK) near Nagycenk, Hungary and in Hylaty, Poland. According to the statistical analysis based on 498 and 946 suitable Q-bursts detected during the surface and underground measurements, respectively, in the Mátra, the average resistivity of the 140 m-thick layer of the Earth's crust above the mineshaft was found to be ~70 Ωm with frequency components considered within the 2–140 Hz range (Figure 1). Skin depths of 1470 m, 1100 m, and 920 m were found at frequencies of 7.8 Hz, 14.1 Hz, and 20.0 Hz corresponding to the first, second, and third Schumann resonance modes, respectively. The advantage of using Q-bursts in surveying the properties of the Earth's crust by electromagnetic (EM) methods is that these natural signals are of high signal-to-noise ratio and the electrical properties of their source can be determined by independent methods. (doi:10.1109/TAP.2022.3161504)

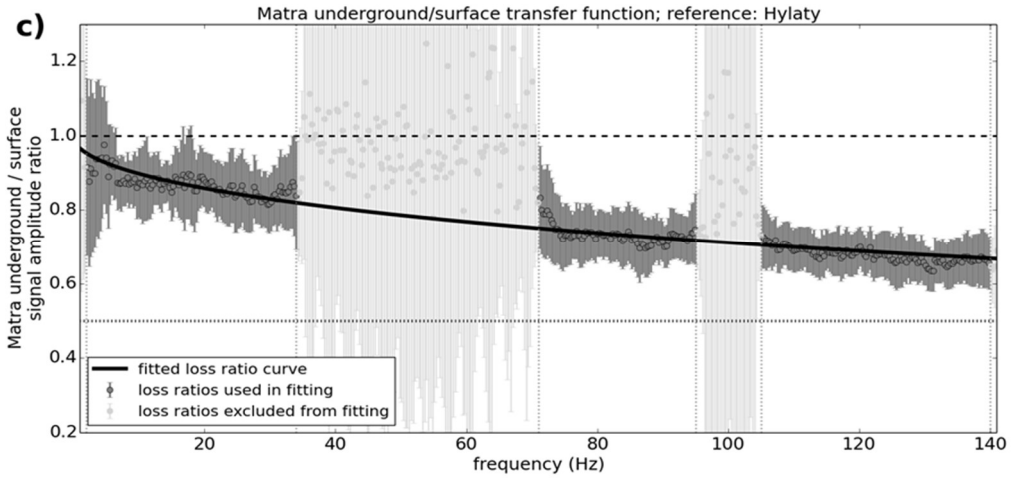

Figure 1. Frequency-dependent attenuation rate of ELF-band signals at 140 m depth in the Mátra mountains, Hungary. Source: Bór et al., 2022.

A new description of our inversion algorithm aimed to reconstruct global lightning activity based on Schumann resonance (SR) measurement has been published (Prácser and Bozóki, 2022) with a strong emphasis on describing quality indicators of the singular value decomposition-based inversion technique. The inversion is tested on synthetic data and the reliability of the obtained results is examined based on the described quality indicators. (doi:10.1016/j.jastp.2022.105892)

After a 14-year break, a new volume (Bozóki et al., 2021a) has been added to the Geophysical Observatory Reports (GOR) series published by the Institute of Earth Physics and Space Science since 1957. The volume consists of a Foreword on the SZIGO and 7 scientific papers, mainly written by the staff of the

institute. The papers present scientific results related to geophysical measurements carried out at SZIGO and other sites associated with the institute. A website for the Geophysical Observatory Reports series has been created and can be accessed via the following link: https://gor.epss.hu/en. The new website not only contains the two new volumes (in English and Hungarian), but also all previous publications in English and German, broken down by studies.

A group of trees located nearby the atmospheric electric potential gradient (PG) measurement site at NCK was cut down on the 24th February in 2020. A study was published in the latest GOR volume about the effect of the change in the electrostatic shielding effect caused by the removal of the trees (Buzás and Bór, 2021). It was found that the PG increased by up to 52% after the trees in question were cut down. Based on numerical model calculations this enhancement was expected to be larger, 78%. Further investigations concerning the seasonal variation of the PG recorded in 2017–2021 affirm that this increase is not part of the regular seasonal variation of the PG and it is an anomaly most likely caused by the diminished electrostatic shielding effect due to the fewer remaining trees. (doi:10.55855/gor2020.1)

A detailed noise test was carried out in the SZIGO in order to survey the electromagnetic noises generated in the ELF band by different electrical devices operating in the observatory. The results of the noise test are described in Bozóki et al. (2021b). (doi:10.55855/gor2020.2)

ELF field measurements were organized to survey the observability of SRs and properties of the ELF noise environment in the magnetic field in Hungary (Bozóki et al., 2021c). The measurements served our aim to find an appropriate location for a new permanent magnetic SR station. Initial evaluation of the field measurements confirmed that it is not easy, but possible to find places of such low ELF noise levels in Hungary, which are suitable for monitoring SR. (doi:10.55855/gor2020.3)

ELF data recorded in the SZIGO is automatically displayed on the website of the observatory (http://nckobs.hu/data/sr/) from July 2020 (Szabóné André et al., 2021). The automatically generated figures contain the dynamic spectra of the H_{NS}, H_{EW} and E_Z field components as well as the amplitude and frequency of the first three SR modes as extracted by the complex demodulation algorithm from the E_Z record. (doi:10.55855/gor2020.5)

A remotely manageable optical observation system for recording transient luminous events in the upper atmosphere was installed in Baja, Hungary in 2014. The report by Bór et al. (2021) describes hardware components and settings of the system, software solutions applied either for realtime event detection and remote control, and the strategy of actually making the observations. An overview on the number and type of TLEs observed up to 2020 is presented. During the 7

years of operation, 1655 TLEs were recorded, 92.7% of which were red sprites, 6.4% were sprite halos, and the set of captured events contained altogether only 3 ELVES. Most sprites were observed in June while most sprite halos were observed in September over the years covered in this report. (doi:10.55855/gor2020.7)

A meteorological station supports other measurements which are running in the observatory. It was located near the so-called ionosonde house surrounded by trees. The station was moved to a more open area, next to the PG measurements on 1st March 2022. Three new instruments were also installed: a LIDAR ceilometer, a present weather and visibility sensor and a barometer. Some plots of the meteorological station's data can be found in the website of the observatory (http://nckobs.hu/data/met/).

*L*aboratory of Lightning Physics and Protection Engineering, State Key Laboratory of Severe Weather, Chinese Academy of Meteorological Sciences, Beijing, China

Association of lightning occurrence with precipitation cloud column structure at a fixed position. Observation data from a C-band frequency-modulated continuous-wave (C-FMCW) radar were combined with lightning data to analyze the relationship between the occurrence of lightning and the structure of precipitation cloud column (PCC) from the perspective of a fixed location. The results show that, relative to PCCs without lightning, PCCs with lightning exhibit greater maximum reflectivity, maximum upward radial velocity, maximum velocity spectrum width, cloud top height, and vertically integrated liquid in terms of their average values, and wider-range distributions of these parameters. Using the Light Gradient Boosting Machine algorithm, a lightning diagnosis program that integrates multiple C-FMCW radar parameters was developed. Its hit rate of lightning occurrence is 93.5% and it has a threat score of 0.421. The maximum velocity spectrum width above the melting layer was found to be the most effective in distinguishing PCCs with or without lightning. The analysis combining the C-FMCW radar and polarimetric radar data indicated that, in a PCC, the hydrometeor properties including the size diversity and content of ice-phase particles should be more important than the convection intensity in diagnosing the occurrence of lightning. The PCCs with lightning have higher ice water content and liquid water content, and

more abundant and larger-size particles (such as graupel particles) than those without lightning.

Close observation of the evolution process during initial stage of triggered lightning based on continuous interferometer. The discharge signal in the initial stage of lightning is weak. The revelation of the discharge mechanism at this stage depends especially on close observation. In this study, a continuous interferometer (CINTF) was used to observe the initial stage of the upward positive leader (UPL) of the triggered lightning in Conghua District, Guangzhou City, Guangdong Province. The positioning error of CINTF for a close-range radiation source was analyzed, and the positioning error calibration method of CINTF for a specific close-range radiation source was studied, which improved the observation accuracy of elevation angle at the initial stage of the UPL of the triggered lightning. With the rise of the rocket, the positioning error in altitude during the initial stage of the UPL increased obviously. Under the layout condition of the Guangzhou field experiment site for lightning research, when the positioning results of the elevation angle of the initial stage of the UPL were 40°, 50°, and 60°, respectively, the calibrated altitude positioning error could be reduced by about 11 m, 14 m, and 20 m, respectively. On the basis of the calibrated observation results, the evolution characteristics of the initial stage of the UPL were studied, and its discharge mechanism was revealed. The precursor current pulse (PCP) was generated by a weak upward positive breakdown and a subsequent strong downward negative breakdown near the rising rocket tip, which was in the form of a single pulse. The precursor current pulse cluster (PCP cluster) and initial precursor current pulse cluster (IPCP) were both signs of self-sustaining development of the UPL. After the PCP cluster, self-sustaining development stopped immediately. The self-sustaining development after IPCP could be short-term or continuous.

Characteristics of regions with high-density initiation of flashes in Mesoscale Convective Systems. To investigate the characteristics of regions exhibiting multiple lightning initiations within a finite volume and a short time, the lightning location data obtained from the convective regions of 14 mesoscale convective systems were analyzed in combination with data from radar. In total, 415 out of 5996 radar grids (1 km × 1 km × 0.5 km) were found to initiate more than one flash within 6 min. Only 49 grids showed an initiation density of more than two flashes within 6 min. The grids with high flash initiation densities were found to have a similar distribution to those with one lightning initiation within 6 min, in terms of altitude and reflectivity relative to altitude (Figure 1). They also showed similar trends in their frequency evolution. The grids with higher initiation densities seemed to be more concentrated in the altitude range of 9–13

km. However, only one was found to form at a lower altitude near the melting level when lightning initiation clearly declined. Moreover, the spatial relationship of this lower higher-initiation density grid to the reflectivity core was different to that in the main altitude range. In this paper, the possible dynamic and electrical mechanisms of the formation of this lower higher-initiation density grid are discussed.

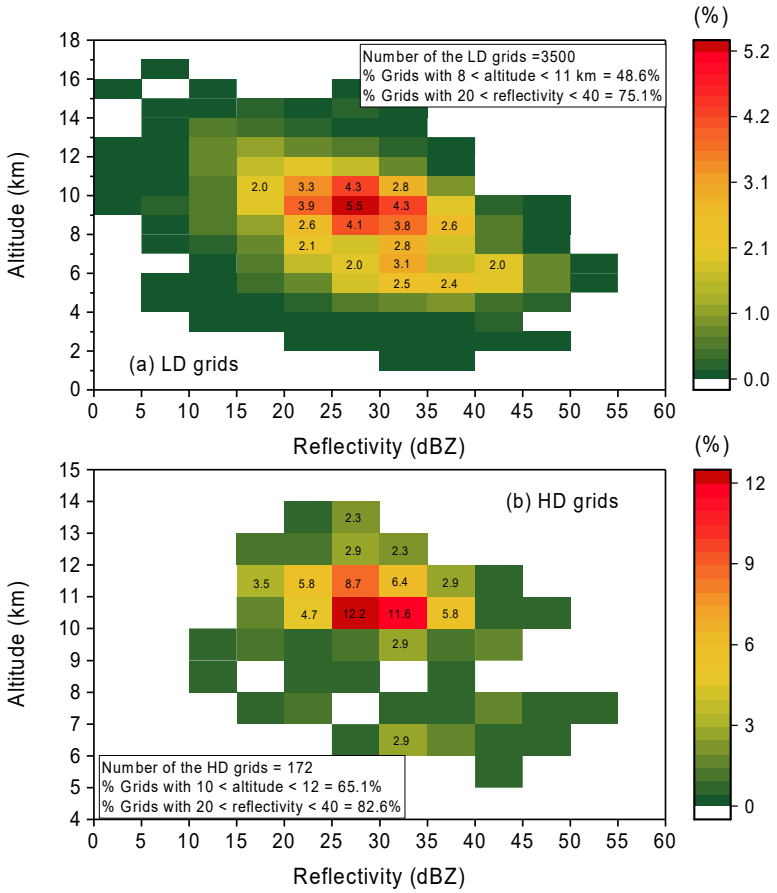

Figure 1. Two-dimensional histogram of the (a) LD (initiation density = 1 flash grid^{-1} 6 min^{-1}) and (b) HD grids (initiation density > 1 flash grid^{-1} 6 min^{-1}) relative to radar reflectivity and altitude for the 14 MCSs.

Evaluation of lightning prediction by an electrification and discharge model in long-term forecasting experiments. Over nearly three rainy seasons of lightning activity in North China, numerical prediction experiments were carried out using the Weather Research and Forecasting model coupled with electrification and discharge schemes (WRF-Electric). The numerical forecast results were evaluated using the neighborhood-based equitable threat score (ETS) and fraction skill score (FSS) verification methods based on nationwide observational lightning data. An algorithm was used to generate the coverage of the total flash

(intracloud and cloud-to-ground flashes) by fitting the cloud-to-ground flash data. The numerical results showed that the region of lightning activity could be well predicted by the mesoscale WRF-Electric model, particularly during a 6–12-hour forecasting period. The average ETS score of the 6–12-hour forecasting period was 0.34 for a 20 km neighborhood radius. The predictive skill of the model varied not only monthly but also diurnally. The model showed better forecasting skills during the main rainy season (June–July–August) and at 14: 00–20: 00 local time. The predictability of the model was enhanced with increasing thunderstorm scale. On the other hand, the coverage of predicted lightning activity was relatively concentrated, and the lightning flash density was higher than the observations. The main discrepancies in the model prediction were related to the design of the discharge parameterization. Thus, in discharge parameterization, the initial threshold for lightning should be modified according to the model resolution, while the magnitude of the neutralization charge in a single discharge should be referenced to the observational results.

New insights into the correlation between lightning flash rate and size in thunderstorms. Data from the Tropical Rainfall Measuring Mission (TRMM) satellite indicate that the flash rate and size in thunderstorms over the Tibetan Plateau (TP) are both lower than in those over the Central and Eastern China (CEC), and much smaller than and analogous to those over the southern foothills of the Himalayas (SHF), respectively. This disagrees with the previously suggested negative correlation between flash rate and size in thunderstorms with different dynamic intensities. This study shows that the TP thunderstorms featuring the weaker convection than those over the other two regions have small vertical and horizontal extents and low charging rate, resulting in the effective charge region (ECR) to be small in size and number, and in turn leading to the coexistence of low flash rate and size. The CEC and SHF thunderstorms with stronger convection causing larger charging rate and more ECRs relative to the TP thunderstorms exhibit a negative correlation between flash rate and size. We deduce that the negative correlation between flash rate and size may only be established when the convection intensity of the compared thunderstorms exceeds a certain threshold. Below the threshold, the increase of dynamic intensity will cause synchronous increase of flash rate and size.

Optical characteristic of needles in a positive cloud-to-ground lightning flash. High-speed video data were used to analyze the initiation and propagation of 36 needles and their associated 306 flickering events observed in a single-stroke positive cloud-to-ground (+CG) flash. The needles occurred during the return-stroke later stage and the continuing current, within approximate 10 ms after the

onset of the +CG return stroke. They initiated near the lateral surface of the predominantly horizontal channel and extended almost perpendicular to that channel. Flickering events are recoil type streamers (or leaders) that retrace the channels created by needles. Flickering events can be repetitive and are classified into four categories based on different scenarios of their occurrence. Needles are caused by the radial motion of negative charge from the hot core of the positive-leader channel into the positive corona sheath surrounding the core, when the core is rapidly recharged (its radial electric field reversed) by the return-stroke process and during the following continuing current (Figure 2).

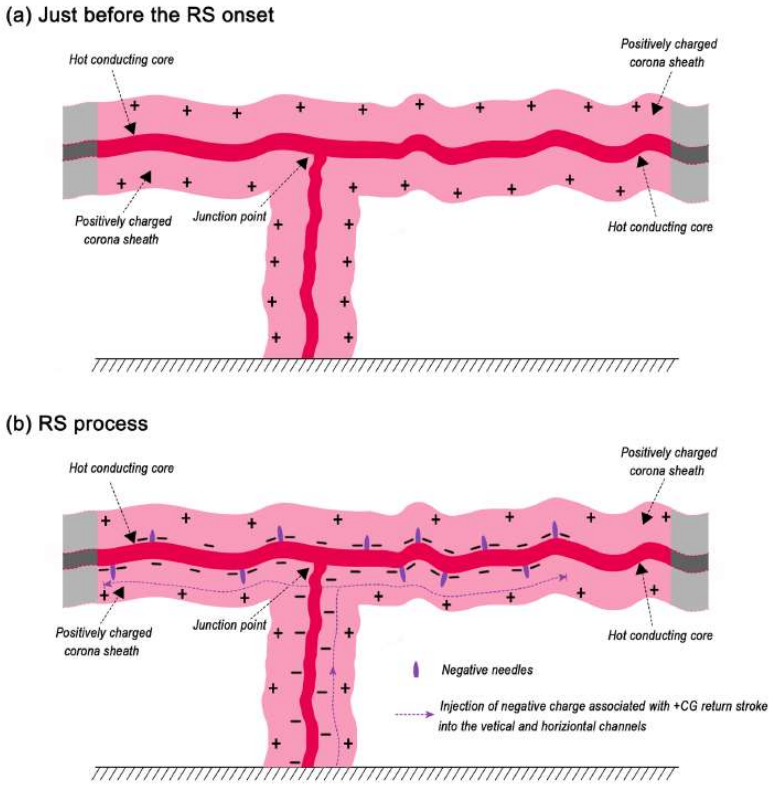

Figure 2. Schematic representation (not to scale) of the likely initiation mechanism of needles originating near the lateral surface of the hot core of the horizontal channel during the return stroke (RS) later stage and the following continuing current, within approximate 10 ms after the onset of the positive cloud-to-ground RS. "+" refers to positive charge and "-" refers to negative charge.

Return-stroke current measurement at the 600-m high Canton Tower. In 2021, the lightning current on the Canton Tower was measured directly for the first time, using a Rogowski coil installed at a height of 492 m above ground level (Figure 3). Return-stroke current measurements for three single-stroke downward negative flashes and two multiple-stroke upward negative flashes were preliminarily analyzed by combining the

associated return-stroke luminosity and data of the lightning location system (LLS). The 10-90% rising time and the full width at half maximum (FWHM) of the first-stroke current were within a range of 6.0 to 9.3 μs and 68.1 to 96.9 μs, respectively. Subsequent-stroke currents were characterized by distinct sharp double peaks, and the typical 10-90% rising time of the initial peak was about 0.4 to 0.5 μs. The FWHM of the subsequent-stroke current ranged from 6.1 to 39.3 μs with AM (GM) value of 18.1 (15.0) μs. An approximately quadratic relation was found between the maximum peak current and the initial peak luminosity for subsequent strokes in the same upward flash. A total of 88% (14/16) of the subsequent strokes were misclassified as intro-cloud (IC) events by the LLS. The LLS-inferred peak current was overestimated by a larger factor for subsequent strokes than the first strokes.

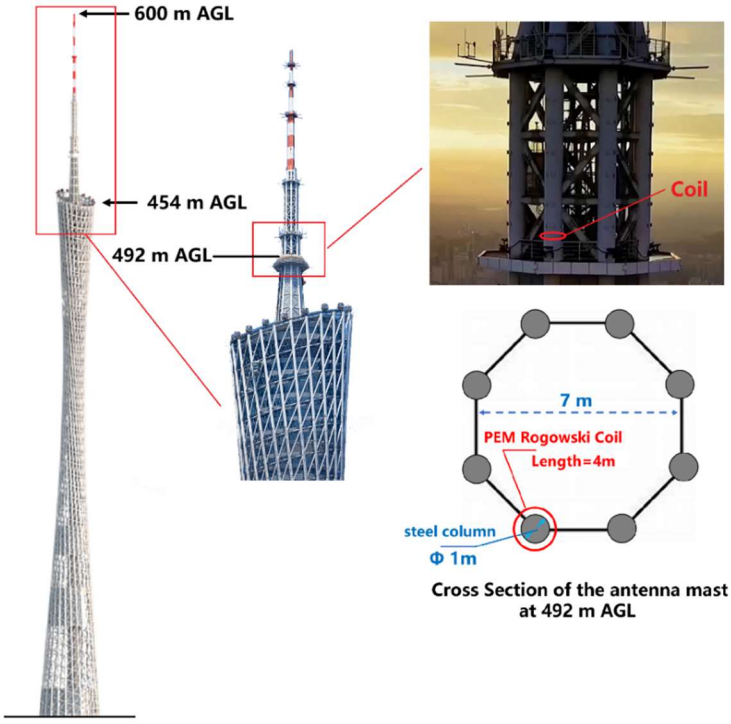

Figure 3. Diagram for the placement of the PEM Rogowski coil on the Canton Tower.

*L*ightning Research Group of Institute of Atmospheric Physics, Chinese Academy of Sciences (IAP, CAS), Beijing, China

Lightning climatology across the Chinese continent from 2010 to 2020. Understanding the lightning climatological distribution is of great significance but remains challenging which is in part due to the lack of continuous and uniform lightning observations. In this paper, for the first time, an 11-year ground-based cloud-to-cloud lightning dataset of China National

Lightning Detection Network from 2010 to 2020 is used to investigate the lightning climatology over China's land area in terms of spatial distribution, seasonal, monthly and diurnal variations. Lightning activity in China's land area generally decreases from south to north and from east to west. The mean cloud-to-ground lightning density of China's land area is 0.9 fl km^{-2} yr^{-1}, with the average maximums (exceeding 10 fl km^{-2} yr^{-1}) are found in the south and east coastal provinces, such as Guangdong, Hainan, Fujian and Zhejiang Province. The lightning activity in spring, summer and autumn seems consistent throughout the daytime cycle, with the lightning activity is rather weak in the morning and most active in the afternoon, while winter lightning appears to be more active in the nighttime and in the very early morning produced from nocturnal thunderstorms. The cloud-to-ground lightning activity in the tropical and subtropical areas within 15–25°N is mainly concentrated in the late spring and early summer, with two weak peaks in May and August, while lightning in mid latitudes within 25–55°N mainly occurs in the summer (June–July-August). The percentage of positive cloud-to-ground lightning flashes with peak current higher than 75 kA is more than 3 times than that of negative cloud-to-ground lightning flashes. Meanwhile, the mean peak current of cloud-to-ground lightning flashes shows an inverse diurnal pattern to the cloud-to-ground lightning activity.

Lightning nowcasting with an algorithm of thunderstorm tracking based on lightning location data over the Beijing area. A thunderstorm tracking algorithm is proposed to nowcast the possibility of lightning activity over an area of concern by using the total lightning data and neighborhood technique. The lightning radiation sources observed from the Beijing Lightning Network (BLNET) were used to obtain information about the thunderstorm cells, which are significantly valuable in real-time. The boundaries of thunderstorm cells were obtained through the neighborhood technique. After smoothing, these boundaries were used to track the movement of thunderstorms and then extrapolated to nowcast the lightning approaching in an area of concern. The algorithm can deliver creditable results prior to a thunderstorm arriving at the area of concern, with accuracies of 63%, 80%, and 91% for lead times of 30, 15, and 5 minutes, respectively. The realtime observations of total lightning appear to be significant for thunderstorm tracking and lightning nowcasting, as total lightning tracking could help to fill the observational gaps in radar reflectivity due to the attenuation by hills or other obstacles. The lightning data used in the algorithm performs well in tracking the active thunderstorm cells associated with lightning activities.

Activation of abundant recoil leaders and their promotion effect on the negative-end breakdown in an intracloud lightning flash. A

unique intracloud lightning flash with multiple positive leader branches spreading out from the same point is studied using simultaneous high-speed images, electromagnetic (EM) field changes, and radiation source mapping. A channel of the positive leader protruded from the cloud and induced a bidirectional luminous segment at tens of meters ahead of the leader tip. They led to a small-scale attachment where multiple channels successively emerged and propagated toward diverse directions. The propagation mode of the positive leader experienced a noticeable transition from stable and smooth channel extension to active development accompanied with frequent recoil leaders, attribute to the arrival of an impulsive current wave induced by the in-cloud activity. We find solid evidence that long recoil leader activated the negative-end breakdown with a regular EM pulse train. The back-and-forth interaction from the opposite ends of the associated channel is revealed (Figure 1).

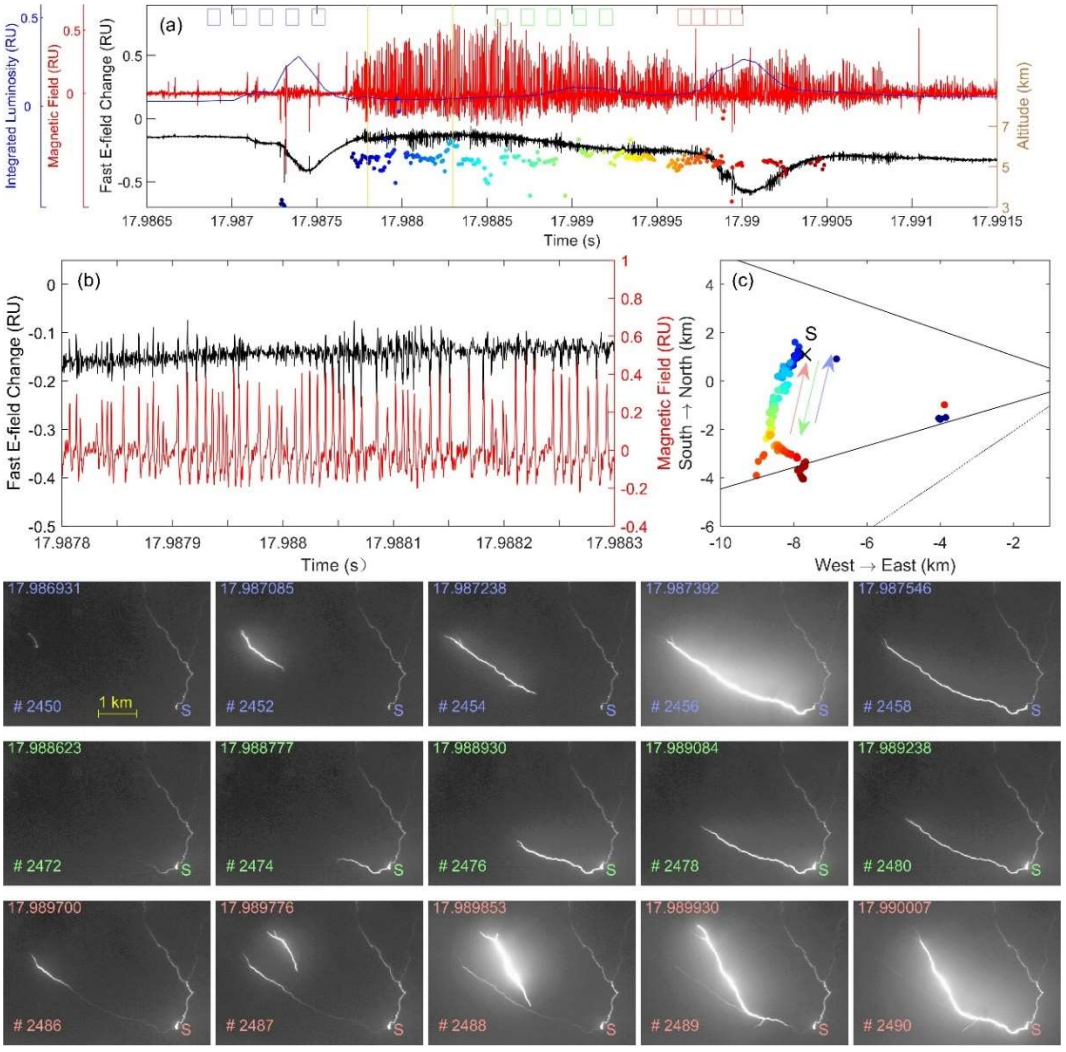

Figure 1. Recoil leader development that retraced an established channel (optical images) and it activates the in-cloud breakdown process thereafter (location results).

Discharge characteristics of upward negative precursors in positive triggered lightning. By using comprehensive data obtained in rocket-triggered lightning experiment, upward negative precursors at the triggering wire tip as during the ascent of the rocket were studied. Except for those typical precursors with peak current of tens of amperes, abundant of weak current pulses were recognized, attributed to the high vertical resolution current detection. All the isolated current pulses were found to be of the weak ones, and all those typical-intensity precursors (or clustered precursors) were preceded by the weak current pulses, involving a time interval of about 20 μs. For the weak pulses, the impulsive pulses and ripple pulses, we obtained their geometric mean values of peak current (3.6 A, 32.2 A, 11.1 A), rise-time from 10% peak to 90% peak (0.39 μs, 0.9 μs, 3.2 μs), duration (2.8 μs, 5.1 μs, 12.7 μs) and charge transfer (4.7 μC, 50.8 μC, 83.2 μC). The typical-intensity precursors formed visible discharge channels that can be detected by optical means, and the channel development of those clustered precursors involved stepwise features consistent with the initial sustained upward leaders, with average 2-D speed in the order of 10^5 m/s. The temporal and spatial relationship of adjacent precursor-producing channels was analyzed. The new precursor channel was found to initiate at the height of the previous channel tip. The significant adjustment of charge distribution due to the stepped channel extension reduced the electric field intensity in the channel region. The precursors were actually un-sustained leader development, which produced initial leader channel segment at the triggering wire tip but eventually extinguished due to the insufficient conditions.

Effects of convective mergers on the evolution of microphysical and electrical activity in a severe squall line simulated by WRF coupled with explicit electrification scheme. To investigate the process of convective merger (CM) and its effect on thunderstorms evolution and corresponding electrical activity, a severe squall line that took place on 27 July 2015 over the Beijing Metropolitan Region (BMR) is simulated and studied using the Weather Research and Forecasting model coupled with an explicit electrification lightning scheme (E-WRF). The model-simulated radar reflectivity reasonably captured the whole squall line evolution, including the merging of individual cells and storms. The variation of normalized flash frequency simulated by E-WRF is highly consistent with the occurrence of a prominent flash rate surge during the CM both in the observation and the simulation. Cloud bridge is one of the regions where lightning events increase most. The upstream anvil and the sinking outflow led to the rapid connection and formation of new convective cells between the two older main storms. Subsequently, the mass of graupel and snow increased substantially at

the middle level, and the mass of upper-level ice was horizontally advected from upstream. During the merger, the in-cloud charge distribution evolved from a staggered charge pocket structure into a vertically stratified five-layer structure. This paper supports the hypothesized role of CM in enhancing lightning activity, and further expands our understanding of CM effects on the microphysical and charge-redistribution.

*M*assachusetts Institute of Technology

Work relating to the polarity of Thunderstorm Ground Enhancement (TGEs) with the vertical development of radar reflectivity overhead in Armenia has now been published in the Journal of Geophysical Research. More recently, investigation by Hripsime Mkrtchyan has revealed some examples of strong 'negative' TGEs characterized by weak reflectivity (<20 dBZ) which appear to originate in debris clouds from earlier, more lightning-active convection. This work is slated for presentation at the upcoming ICAE in Tel Aviv.

A newly designed device for the measurement of electric field and ionospheric potential by balloon is currently under development with Quasar in San Diego under NSF sponsorship. When the new instruments are available, simultaneous balloon soundings are planned from Graciosa Island in the Atlantic Ocean and from New Zealand in the Pacific Ocean, roughly 180 degrees apart in longitude, and so sampling opposite phases of the local diurnal cycle.

Long discussion (~ 3 years) among Heon Kang, Rohan Jayaratne and Earle Williams has led to the recent submission to JGR with a proton-based mechanism for charge separation in ice particle collisions in thunderstorms. The work addresses shortcomings in earlier suggested mechanisms. The relative growth rate hypothesis of Baker et al. (QJRMS, 1987) has been a guiding influence on the macroscopic scale.

Collaboration among Hungarian investigators, Vaisala Inc, and the HeartMath Institute on the superlative January 15, 2022 eruption at Tonga has shown that this event produced more lightning (for a period of at least one hour near 0500 UT) than all the other lightning on Earth. This work is in preparation for publication.

Reichman University

Yoav Yair, Roy Yaniv (Reichman University) and Colin Price (Tel-Aviv University) conducted successful lightning and TLE observations from the International Space Station during the Rakia mission, that took place April 8-25th 2022. In the framework of the ILAN-ES campaign, Mr. Eytan Stibbe, the 2nd Israeli astronaut on-board the private AX-1 flight, received daily targets towards which he directed the Nikon D6 camera, which was equipped with a 50 mm lens. The daily thunderstorm forecasts were aided by inputs from Eliah São-Sabbas from INPE, specifically for South America. Approximately 2 hours of usable data had been received, and initial analysis shows good results of high-resolution, full color images of ~20 different TLEs – sprites, Elves, Halos and Blue Corona Discharges (Figure 1). These events will be compared with parent lightning properties, derived from international networks such as ENTLN and GLD360, in collaboration with Olivier Chanrion from DTU.

Figure 1. A team of students from Reichman University worked on ground-based observations with 15 schools in Israel, Africa and Asia, to support the mission with optical cameras model Watec 06U2D. This educational project helped increase awareness to lightning safety in those schools.

Yoav Yair (Reichman University) and Barry Lynn (Hebrew University of Jerusalem) continue their research on lightning superbolts in the eastern Mediterranean region. The climatology of east-Mediterranean super-bolts (peak current > 200 kA) occurring in winter thunderstorms (DJF) for the period 2018-2022 was completed, and a comparison of data obtained by various lightning detection networks (ENTLN, WWLLN and ILDN) was conducted. There are some clear superbolts "hot-spots" over the Mediterranean Sea, close to the coasts of Egypt, Lebanon and Turkey. Winter storms sometimes exhibit a larger percentage of superbolts compared with the global average, up to 0.65% of total flashes. The WRF-ELEC code was being updated in order to simulate winter thunderstorm in the area and to study the effects of desert dust. The approach is to calculate charging among hydrometeor particles, and then from them to calculate bulk values associated with each hydrometeor type. These bulk values are then used as input into the Electrical Field Calculator of WRF-ELEC, and then are discharged using various approaches to calculating lightning events. Results of the simulations will be presented in future publications.

*U*niversity of Florida

Z. Ding and V.A. Rakov authored a paper titled “Toward a Better Understanding of Negative Lightning Stepped Leaders”, which is based on (is an extended version of) the Keynote Speech given by the authors at the GROUND 2020/21 & 9th LPE in Belo Horizonte, Brazil. The authors found that negative lightning leaders observed at very close (within a few kilometers) distances often exhibit heavy branching with many active tips forming a network-like structure with a descending multi-tip “ionization front” whose transverse dimensions are of the order of hundreds of meters. The presence of such front makes the lightning attachment process more complex than usually assumed. Negative leader branches extend in a step-like manner, with each step necessarily generating a traveling wave moving positive charge from the branch tip up along the channel, like a mini return stroke. The leader stepping process has a number of generally unrecognized consequences. Specifically, a stepped-leader branch tip can collide with the lateral surface of an adjacent branch (usually at an angle of about 90°). Further, branches formed at earlier negative leader stages (at higher altitudes) may lose their connection to the main channel and decay (become non-luminous). Stepping-related waves moving positive charge from the leader tip up along the hot leader channel can reactivate decayed

negative branches at higher altitudes, possibly via cumulative effect of stepping at multiple active leader tips. Overall, a heavily-branched negative stepped leader creates a highly-structured and rapidly-changing electric field pattern inside and in the vicinity of the volume it occupies, which causes complex interactions between the branches. The paper is published in the Special Issue of Electric Power Systems Research (EPSR) devoted to GROUND 2020/21 & 9th LPE.

I. Kereszy, V.A. Rakov, Z. Ding, and J.R. Dwyer authored a paper titled "Ground-based observation of a TGF occurring between opposite polarity strokes of a bipolar cloud-to-ground lightning flash", in which they presented the ground-based observation of a terrestrial gamma-ray flash (TGF) that occurred between positive (second) and negative (third) strokes of a five-stroke bipolar cloud-to-ground lightning flash. Those two strokes shared the same channel to ground at a distance of 200 m or so from the Lightning Observatory in Gainesville (LOG), Florida. Earlier TGF observations at ground level in Florida (a total of four) were either associated with the initial continuous current (ICC) of rocket-triggered lightning flashes or occurred during the relatively steady current following the return-stroke current peak in natural lightning flashes; that is, in the presence of current-carrying channel to ground. The TGF presented in this paper occurred in a different context: at the early (in-cloud) stage of negative leader entering the remnants of the channel previously created by the positive stroke. The TGF had a duration of 35 μs and consisted of 18 pulses with amplitudes ranging from 114 to 912 keV. The authors compared the various scenarios of acceleration and multiplication of runaway electrons in terms of the source of seed electrons, air temperature, and characteristic electric field (see Table below), with conventional (non-relativistic) avalanches being additionally included as a reference. Results of this study provide support to the elevated-temperature scenario, which requires realistic (confirmed by modeling) electric fields and no energetic electrons from external sources. The paper is published in the JGR-Atmospheres.

Process	Source of seed electrons	Air temperature, K	Electric field, MV/m
Relativistic avalanches in cold air (cold runaway breakdown)	Two-step process starting with ambient distribution	300	≳30
Relativistic avalanches in cold air (RREA)	Cosmic-ray secondaries	300	~0.2
Relativistic avalanches in remnants of decayed channel	Ambient distribution	3,000	≳3
Conventional (non-relativistic) avalanches in cold air	Ambient distribution	300	~3

Electric fields in the last column are approximate values at sea level.

University of Toulouse, France

Thunderstorm electrification and aerosol: abnormally charged structures. Since summer 2014, the SAETTA lightning imager network is continuously operated in Corsica, within the framework of the CORSiCA Platform of Atmospheric Observations (PCOA), thanks to the support of the University Toulouse III - Paul Sabatier (UT3), the National Institute of Sciences of the Universe (INSU), the National Center for Scientific Research (CNES), and the Collectivity of Corsica. The SAETTA observations analyzed over the period 2014-2019 on a domain of 240 km x 240 km, centered on Corsica, show a very clear maximum of activity on the center of the island, above the crossroads of the 3 main valleys, specifically in summer from 12:00 to 14:00 (Coquillat et al., 2022). This maximum appears under the effect of the diurnal convection, probably fed by the convergence of low layer of humid air, induced by the sea breezes channeled by these 3 valleys. The autumn is also prone to a very strong electrical activity associated with organized mesoscale systems, most often over the sea. The month of September presents, as such, the largest monthly number of days of thunderstorms, with a remarkable consistency from year to year.

The 3D observation allows describing the electrical structure of the thunderstorm cells which is most of the time of tripolar form in this region. They are indeed made up of a main pole of positive charge associated with ice crystals at the upper level, a main pole of negative charge associated with the graupel at the intermediate level, and a secondary pole of positive charge associated with the precipitation at the lower level. However, anomalously electrified thunderstorms have been observed. These ones are characterized by a negative dipole structure (i.e. a negative charge at the upper level and a positive charge at the lower level) of small horizontal dimensions with a moderate vertical development. These atypical storms move almost linearly over long distances (up to 230 km) with a very rapid speed between 80 and 90 km h^{-1} (more than 100 km/h for some). Remarkably, all of them take place during strong wind episodes with a South to South-West flow.

The analysis of these events was based on the documentation of (i) the aerosol environment (GEOS-5, CAMS Copernicus, AERONET) and (ii) of the meteorological environment (numerical simulations of the ARPEGE and AROME meteorological models in collaboration with the Ecole Nationale de la Météorologie) These events are associated with a strong transport of large desert dust from the African continent (Figure 1), a relatively cold temperature at the ground, a dry low layer, and a convection triggered above the boundary layer in an air containing relatively little water vapor.

The different hypotheses (microphysical and radiative) put forward to explain these events lead to a low content of cloud liquid water at the origin of an unusual electrification according to the non-inductive charging process.

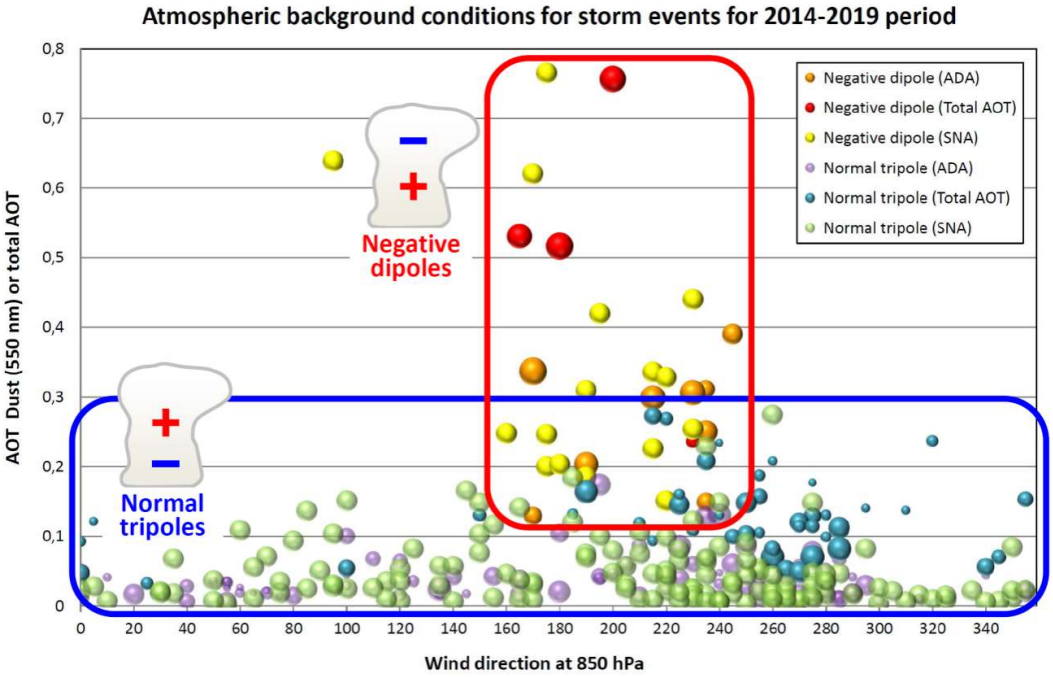

Figure 1. Aerosol Optical Thickness for dust aerosols (AOT Dust) versus wind direction at 850 hPa for the whole lightning event dataset over the 2014–2019 period. The red, orange and yellow spheres represent the negative dipoles. The blue, purple and green spheres represent normal tripoles. The sphere size is a proxy of the aerosol size contributing mainly to the AOT. ADA: All Data Available (AOT Dust, Wind direction and proxy of size). Total AOT: all types of atmospheric aerosols from Ersa site available in 2014 and 2015. SNA: Size Not Available, arbitrary size of spheres.

Lightning activity in Congo Basin. The continuation of a collaboration with the University of Kinshasa has made it possible to analyze lightning detection and meteorological data on the territory of the Democratic Republic of Congo, which experiences very intense storm activity throughout the year (Kigotsi et al., 2022). Thus, lightning activity issued from World Wide Lightning Location Network (WWLLN), storm structures with Meteosat observations, meteorological and environmental conditions thanks to reanalysis provided by the European Copernicus/ECMWF Data Center and the US NCEP/NCAR and NOAA, are considered within a large area of Central Africa (25° × 25°) and for two periods of one month (March and December) with high thunderstorm activity in 2013. These periods correspond to the

year with the best detection efficiency and two months with high level of lightning activity and low variability from one year to the next in the database available.

A correlation is found between the daily flash number and the extent of large CAPE values. We note a seasonal effect on the number of flashes produced by storms with the same extent of large CAPE values. There were also large values of moisture in the lower layers of the troposphere in the days with a strong lightning activity. The lightning flash density distribution for each period of one month shows the same location for the maximum, which corresponds to the main maximum reported in the literature for annual activity. The storms developments characterized by the first flash detected often occur in the regions that combine the presence of lakes and mountains, which shows the role of the relief for triggering convection. The flash rate density is larger in the convective systems well organized, as the typical MCS, and when several cells merge. The flash clusters allow to localize the strong convective activity and to follow the displacement of the storm systems when they move.

Contribution to SAINT project. In the frame of SAINT (https://www.saint-h2020.eu/), a study developed at University of Toulouse concerns the physics of several types of TLEs (sprites, elves and halos) and their physical links to the storm and the lightning flash producing them. In this goal, ground and space observations of TLEs are used to investigate the most promising parameters responsible for their production. A statistical analysis of ground observations of nearly 600 TLEs obtained during 2017 from a camera in Pic du Midi, France, has been performed. The main parameters analyzed are the TLE-producing strokes including their peak currents, delay, and current moment, the cloud top temperature (CTT) optical intensities of the thunderstorms, and thundercloud characteristics obtained through image processing techniques. The results obtained from the ground observations include the clear distinction between the types of strokes that produce the different types of TLEs observed: sprites, halos and elves. Zaida Gomez Kuri defended a thesis including the results of this study on October 8th, 2021, that the title is "Analysis of Transient Luminous Events from Ground and Space Observations".

A paper has been published in Geophysical Research Letters journal, about a rarely observed sprite event that displayed 8 simultaneous columns that showed converging luminosity in individual streamer channels lasting up to 160 ms (Gomez Kuri et al., 2021). This observation suggests that detachment of electrons becomes important, driving long-lasting currents in streamer filaments, when there is a continuous current in the parent CG stroke. The current in the streamer filament drives the space charge upward in the positive

(lower) tip and feeds the space charge in the negative (upper) tip of the streamer channel explaining the converging motion of the luminosity. The analytical formulation presented here can be used for modeling the phenomenon in future work.

Thunderstorm producing dancing sprites. A collaboration between the Laero (Serge Soula, Eric Defer, Serge Prieur), the Danish Technical University (Maja Tomicic, Olivier Chanrion, Torsten Neubert, Christoph Koehn), the Polish AGH University of Science and Technology of Krakow (Janusz Mlynarczyk) and the French Atomic Energy and Alternative Energies Commission (Thomas Farges) lead to make a comprehensive analysis of a thunderstorm which produced a very high proportion of dancing sprites in southern France (Tomicic et al., 2021). This long duration MCS storm (20 hr) on September 21st, 2019, produced 21 sprites captured on video of which 19 were of dancing type. The SP+CG flashes and strokes responsible for the sprite initiation, and the whole lightning activity of the storm were analyzed using Radio-Frequency radiations from a VHF LMA (SAETTA), LF and VLF detections from two operational LLS, and CMWs from ELF receiver measurements. CTT and radar data as well as meteorological reanalysis data allowed a comprehensive analysis of the cloud conditions that generated the high amount of dancing sprites.

The SP+CG flashes were of exceptionally long horizontal extent and duration (average of 156 km and 2.9 s, respectively), that is, 3–4 times longer than previously reported values from LMA-based studies. The flashes that triggered the dancing sprites followed a similar propagation pattern where most flashes initiated in the convective region of an asymmetric MCS with a bow echo phase and propagated into the stratiform region. Most sprite sequences (87.5%) were produced by distinct +CG strokes separated in time by tens to hundreds of milliseconds (80% were between 40 and 300 ms). Two sprite sequences were triggered with a short delay after three strokes separated by a very short time (1–3 ms) and a large distance (spanning 32–54 km), which can explain a type of dancing sprite in which the individual sequences are not resolvable at video frame rates of 25 frames/second leading to exceptionally wide and bright sprites (Figure 2). The meteorological conditions that lead to this high proportion of dancing sprites corresponded with large CAPE values of 3,500 J kg^{-1} and wind shear of 20 m s^{-1}, resulting in a large region with cold CTT (2,900 km^2 with CTT < − 66°C) and a high maximum CG flash rate (30–35 fl min^{-1}).

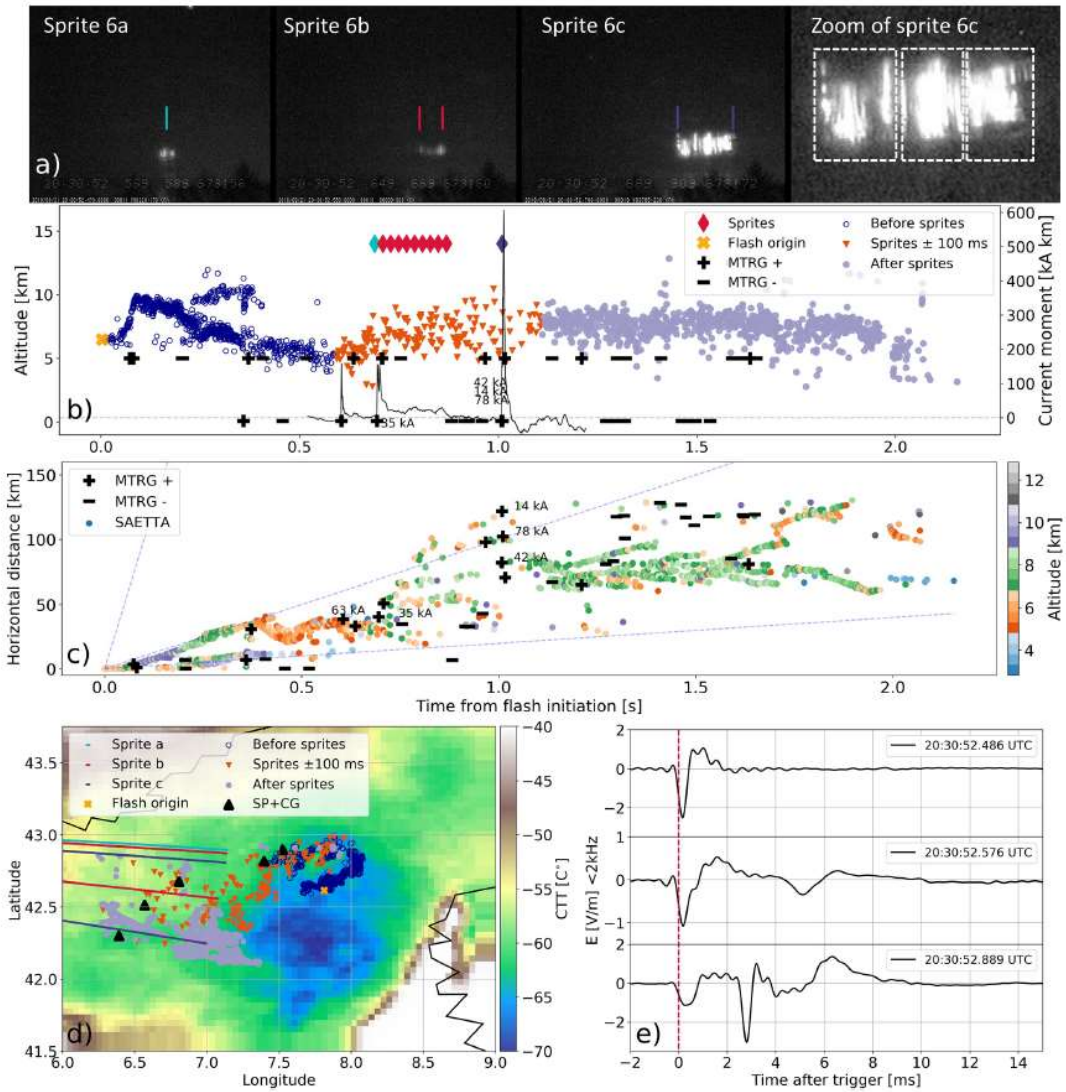

Figure 2. (a) Brightest video field for each sequence of sprite at 20:30:52 UTC, including a zoom of sprite 6c with boxes indicating three distinguishable structures. The lines (one color for each sprite) indicate the location of the line of sight (LOS) from the camera to the sprite reported in panel (d). (b) Altitude of very high frequency (VHF) sources with time. All MTRG detections are shown as pluses and minuses (for positive and negative polarity, respectively) with IC at arbitrary altitude and CG strokes at ground level. Overlaid is the CMW during the sprite production (black curve). (c) Time-distance plot of the parent flash with colors representing altitude. Pluses and minuses are positive and negative polarity MTRG detections. The dashed lines are reference lines for leader speeds. Going from steepest to flattest they are 10^6 m s^{-1}, 10^5 m s^{-1} (typical speed of negative leaders) and 2×10^4 m s^{-1} (typical speed for positive leaders as observed in VHF). (d) Longitude-latitude map. Cloud top temperatures at 20:26 UTC from SEVIRI is shown in colors. The LOS directions of the sprites are

shown in lines with one color for each sprite sequence as explained in the legend. VHF sources from the parent flash are superimposed. Blue open circles are from before the sprites, triangles are during the sprites, gray full circles are after the sprites. (e) Vertical electric field (ELF band) during the event reconstructed from the data recorded by a broadband vertical dipole whip antenna installed in the center of France. Each legend shows the trigger time (i.e., including the signal propagation time of ~2 ms for 700 km distance from storm to antenna) corresponding to t = 0 (red dashed line).

Thunderstorm producing energetic preliminary breakdown. We conducted a study with the Institute of Atmospheric Physics of the Czech Academy of Sciences in Prague (Ivana Kolmašova and Ondrej Santolik), the French Atomic Energy and Alternative Energies Commission (Thomas Farges), the French Lacy of University of la Réunion (Olivier Bousquet) and the Austrian department ALDIS of OVE Service GmbH (Gerhard Diendorfer), after an observation of unusually strong preliminary breakdown (PB) in southern France (Kolmašova et al., 2022). The PB pulses were produced by a multi-cellular thunderstorm system storm that developed along the Mediterranean Coast of Southern France in the early hours of 19 June 2013 and which was composed of several parallel convective lines. Our analysis focused on 10 sequences of energetic electromagnetic PB pulses recorded by two receivers located at different distances from this thunderstorm. The initial polarity of all observed energetic PB pulses confirmed the movement of the negative charge downward, as in cases of PB pulses preceding negative cloud-to-ground discharges. The locations of PB pulses appeared in areas with none or very weak lightning activity. Most PB pulses were initiated in small, short-lived, rapidly moving convective storm cells characterized by low reflectivity values (generally <40 dBZ), weak vertical development (cloud top lower than 10 km), and low flash density (an example is shown in Figure 3). Our interpretation is based on the presence of temporary strong negatively charged pockets located above a strong positive charge region at low-level, within these thunderclouds. Such charge arrangement, later carried down by precipitation, likely explains our observation of unusually strong PB pulses and the absence of RS pulses in electromagnetic recordings.

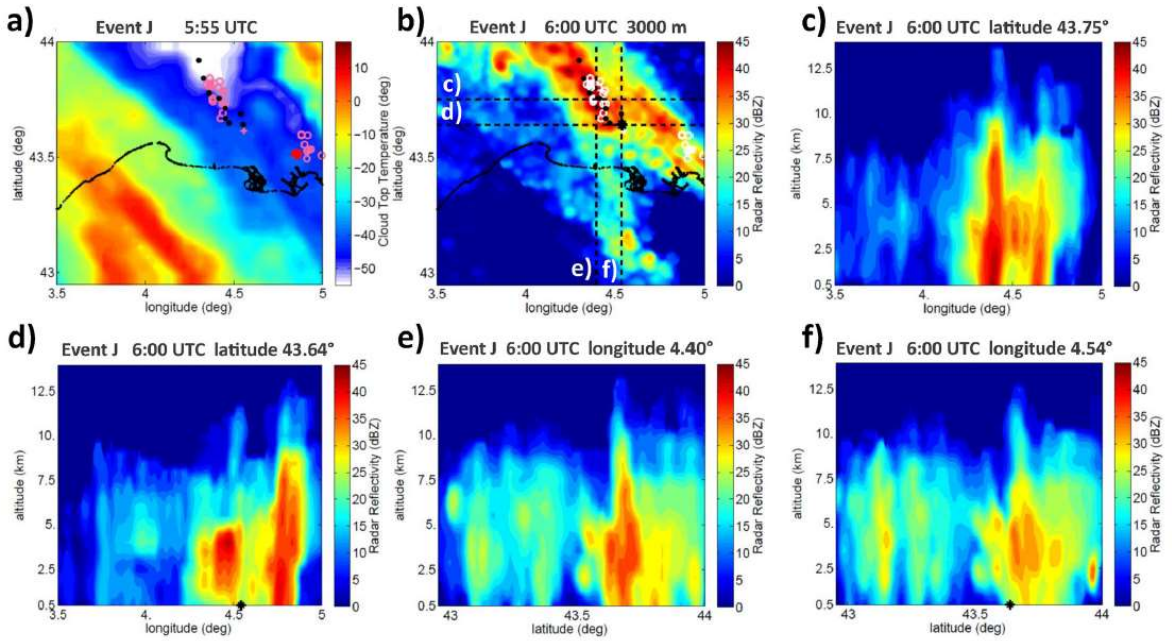

Figure 3. Example of thunderstorm producing an energetic PB pulse: (a) CTT in Celsius at the time indicated; (b) horizontal cross section of radar reflectivity in dBZ at 3,000 m of altitude (from several scans made over 10 min before 06:00 UTC); (c–f) vertical cross section of radar reflectivity along the dashed lines in (b). The strokes (pulses) detected by EUCLID (05:50–06:00 UTC) are plotted in panels a) and b) (white circles for -CG, pink and white pluses for +CG and black dots for IC). The PB pulse is indicated with red and black stars.

RECENT PUBLICATIONS

This list of references is not exhaustive. It includes only papers published during the last six months provided by the authors or found from an on-line research in journal websites. Some references of papers very soon published have been provided by their authors and included in the list. The papers in review process, the papers from Proceedings of Conference are not included.

Andreotti, A., Rakov, V.A., Verolino, L. Modeling of lightning and its interaction with overhead conductors", Ch. 12 in "Advanced time domain modelling for electrical engineering", ed. R. Araneo, IET, London, 2022, pp. 371-399.

Berge, N., Celestin, S., Garnung, M.B., et al. 2022. Modeling low-frequency radio emissions from terrestrial Gamma ray flash sources. J. Geophys. Res. Atmos., 127, e2021JD036040. doi:10.1029/2021JD036040.

Bogatov, N.A., Syssoev, V.S., Sukharevsky, D.I., et al. 2022. An experimental study of the breakthrough-phase and return-stroke processes in long sparks. J. Geophys. Res. Atmos., 127, e2021JD035870. doi:10.1029/2021JD035870.

Bór, J. et al. 2022. Estimating the attenuation of ELF-band radio waves in the Earth's crust by Q-bursts. IEEE T. Antenn. Propag., doi:10.1109/TAP.2022.3161504.

Bór, J., Hegedüs, T., Jäger, Z., et al. 2021. Remotely controlled observations of electrooptical upper atmospheric phenomena from Baja, Hungary. Geophysical Observatory Reports, 2020, 51-65.

Bozóki, T., Bór, J., Novák, A., et al. 2021c. ELF field measurements near Hortobágy and Magyargencs. Geophysical Observatory Reports, 2020, 18-25. doi:10.55855/gor2020.3.

Bozóki, T., Bór, J., Piri, D., et al. 2021b. ELF noise test in the Széchenyi István Geophysical Observatory. Geophysical Observatory Reports, 2020, 14-17. doi:10.55855/gor2020.2.

Bozóki, T., Buzás, A., Szabóné André, K. (eds.) 2021a. "Geophysical Observatory Reports 2020". https://gor.epss.hu/issues/GOR2020.

Buzás, A., Bór, J. 2021. Investigating the impact of cutting down nearby trees on measured values of the atmospheric electric potential gradient data. Geophysical Observatory Reports 2020, 6-13. doi:10.55855/gor2020.1.

Cao, J., Du, Y., Ding, Y., et al. 2022. Lightning surge analysis of transmission line towers with a hybrid FDTD-PEEC method. IEEE T. Power Deliver., 37, 1275-1284.

Chen, H., Chen, W., Wang, Y., et al. 2022. A low computational cost lightning mapping algorithm with a nonuniform L-shaped array: Principle and verification. IEEE Trans. Geosci. Remote Sens., 60, 4106410. doi:10.1109/TGRS.2021.3139388.

Chen, L., Lyu W., Ma, Y., et al. 2022. Return-stroke current measurement at the Canton

Tower and preliminary analysis results. Electr. Pow. Syst. Res., 206, 107798. doi:10.1016/j.epsr.2022.107798.

Chen, Z., Zhang, Y., Fan, Y., et al. 2022. Close observation of the evolution process during initial stage of triggered lightning based on continuous interferometer. Remote Sens., 14, 863. doi:10.3390/ rs14040863.

Chen, Z., Zhou, Q., Du, B., et al. 2022. Electromagnetic transient calculation and protective measures of transformers under lightning overvoltage. IEEE Trans. Dielectr. Electr. Insul., 29,718-726.

Coquillat, S., Pont, V., Lambert, D., et al. 2022. Six years of electrified convection over the island of Corsica monitored by SAETTA: General trends and anomalously electrified thunderstorms during African dust south flow events. Atmos. Res., 275, 106227. doi:10.1016/j.atmosres.2022.106227.

Cui, Y., Zheng, D., Zhang, Y., et al. 2022. Association of lightning occurrence with precipitation cloud column structure at a fixed position. Atmos. Res., 267, 105989. doi:10.1016/j.atmosres.2021.105989.

Dai, B., Li, J., Zhou, J., et al. 2022. Application of a modified empirical wavelet transform method in VLF/LF lightning electric field signals. Remote Sens., 14, 1308. doi:10.3390/rs14061308.

de Vasconcellos, F.M., Alipio, R., Moreira, F.A. 2022. Evaluation of the lightning performance of transmission lines partially protected by surge arresters considering the frequency-dependent behavior of grounding. IEEE Lat. Am. T., 20, 352-360.

Ding, Z., Rakov, V.A. 2022. Toward a better understanding of negative lightning stepped leaders. Electr. Pow. Syst. Res., 209, 108043. doi:10.1016/j.epsr.2022.108043.

Fairman, S.I., Bitzer, P.M. 2022. The detection of continuing current in lightning using the Geostationary Lightning Mapper. J. Geophys. Res. Atmos., 127, e2020JD033451. doi:10.1029/2020JD033451.

Gomez, K., Soula, Z., Neubert, S., et al. 2021. Converging luminosity in columnsprite filaments. Geophys. Res. Lett., 48, e2020GL090364. doi:10.1029/2020GL090364.

Guo, S., Wang, J., Gan, R., et al. 2022. Experimental study of cloud-to-ground lightning nowcasting with multisource data based on a video prediction method. Remote Sens., 14, 604. doi:10.3390/rs14030604.

He, J., Loboda, T.V, Chen, D. et al. 2022. Cloud-to-ground lightning and near-surface fire weather control wildfire occurrence in Arctic tundra. Geophys. Res. Lett., 49, e2021GL096814. doi:10.1029/2021GL096814.

Hessilt, T.D., Abatzoglou, J.T., Chen, Y., et al. 2022. Future increases in lightning ignition efficiency and wildfire occurrence expected from drier fuels in boreal forest ecosystems of western North America. Environ. Res. Lett.,

17, 054008. doi:10.1088/1748-9326/ac6311.

Huang, Y., Fan, Y., Cai, L., et al. 2022. A new thunderstorm identification algorithm based on total lightning activity. Earth Space Sci., 9, e2021EA002079. doi:10.1029/2021EA002079.

Ishimoto, K., Tossani, F., Napolitano, F., et al. 2022. Direct lightning performance of distribution lines with shield wire considering LEMP effect. IEEE T. Power Deliver., 37, 76-84.

Jacobson, A.R., Holzworth, R.H., Brundell, J.B. 2022. Using the World Wide Lightning Location Network (WWLLN) to study very low frequency transmission in the earth-ionosphere waveguide: 2. Model test by patterns of detection/non-detection. Radio Sci., 57, e2021RS007362. doi:10.1029/2021RS007362.

Jiang, R., Yuan, S., Qie, X., et al. 2022. Activation of abundant recoil leaders and their promotion effect on the negative-end breakdown in an intracloud lightning flash. Geophys. Res. Lett., 49, e2021GL096846. doi:10.1029/2021GL096846.

Kahlon, M., Lipshtat, A., Price, C., et al. 2022. Classification of infrasonic atmospheric events using electromagnetic pulse analysis. J. Geophys. Res. Atmos., 127, e2021JD035464. doi:10.1029/2021JD035464.

Kang, N., Bortnik, J. 2022. Structure of energy precipitation induced by superbolt-lighting generated Whistler waves. Geophys. Res. Lett., 49, e2022GL097770. doi:10.1029/2022GL097770.

Kereszy, I., Rakov, V.A., Ding, Z., et al. 2022. Ground-based observation of a TGF occurring between opposite polarity strokes of a bipolar cloud-to-ground lightning flash. J. Geophys. Res. Atmos., 127, e2021JD036130. doi:10.1029/2021JD036130.

Kigotsi, K.J., Soula, S., Kazadi, M.B.A., et al. 2022. Contribution to the study of thunderstorms in the Congo Basin: Analysis of periods with intense activity. Atmos. Res., doi:10.1016/j.atmosres.2021.106013.

Kolmasova, I., Santolik, O., Rosicka, K. 2022. Lightning activity in northern Europe during a stormy winter: disruptions of weather patterns originating in global climate phenomena. Atmos. Chem. Phys., 22, 3379-3389.

Kolmašova, I., Soula, S., Santolik, O., et al. 2022. A frontal thunderstorm with several multi-cell lines found to produce energetic preliminary breakdown. J. Geophys. Res. Atmos., 127, e2021JD035780. doi:10.1029/2021JD035780.

Kolmasova, I., Soula, S., Santolik, O., et al. 2022. Frontal thunderstorm with several multi-cell lines found to produce energetic preliminary breakdown. J. Geophys. Res. Atmos., 127, e2021JD035780. doi:10.1029/2021JD035780.

Lakhdar, A., Mimouni, A., Azzouz, Z.-E. 2022. New approach to revise the spatiotemporal

lightning current distribution models intended for tall objects. IEEE T. Electromagn C., doi:10.1109/TEMC.2022.3169429.

Li, D., Luque, A., Gordillo-Vazquez, F. J., et al. 2022. Secondary fast breakdown in Narrow Bipolar Events. Geophys. Res. Lett., 49, e2021GL097452. doi:10.1029/2021GL097452.

Li, J., Dai, B., Zhou, J., et al. 2022. Preliminary application of long-range lightning location network with equivalent propagation velocity in China. Remote Sens., 14, 560. doi:10.3390/rs14030560.

Lindanger, A., Skeie, C.A., Marisaldi, M., et al. 2022. Production of terrestrial gamma-ray flashes during the early stages of lightning flashes. J. Geophys. Res. Atmos., 127, e2021JD036305. doi:10.1029/2021JD036305.

Liu, N., Scholten, O., Dwyer, J.R., et al. 2022. Implications of multiple corona bursts in lightning processes for radio frequency interferometer observations. Geophys. Res. Lett., 49, e2021GL097367. doi:10.1029/2021GL097367.

Liu, N.Y., Scholten, O., Hare, B.M., et al. 2022. LOFAR observations of lightning initial breakdown pulses. Geophys. Res. Lett., 49, e2022GL098073. doi:10.1029/2022GL098073.

Lopez, J.A., Montanya, J., van der Velde, O., et al. 2022. Initiation of lightning flashes simultaneously observed from space and the ground: Narrow bipolar events. Atmos. Res., 268, 105981. doi:10.1016/j.atmosres.2021.105981.

Lu, M., Zhang, Y., Chen, M., et al. 2022. Monitoring lightning location based on deep learning combined with multisource spatial data. Remote Sens., 14, 2200. doi:10.3390/rs14092200.

Ma, M., Huang, X., Fei, J., et al. 2022. Analysis of the winter cloud-to-ground lightning activity and its synoptic background in China during 2010-20. Adv. Atmos. Sci., 39, 985-998.

Machado, J.G.O., Hare, B.M., Scholten, O., et al. 2022. The relationship of lightning radio pulse amplitudes and source altitudes as observed by LOFAR. Earth Space Sci., 9, e2021EA001958. doi:10.1029/2021EA001958.

Maiorana, C., Marisaldi, M., Füllekrug, M., et al. 2021. Observation of terrestrial Gamma-ray flashes at mid-latitude. J. Geophys. Res. Atmos., 126, e2020JD034432. doi:10.1029/2020JD034432.

Mallick, C., Hazra, A., Saha, S.K., et al. 2022. Seasonal predictability of lightning over the global hotspot regions. Geophys. Res. Lett., 49, e2021GL096489. doi:10.1029/2021GL096489.

Paul, C., Heidler, F.H. 2022. Simultaneous upward lightning from small structures and from the 150-m high Peissenberg Tower, Germany. IEEE T. Electromagn C., doi:10.1109/TEMC.2022.3168491.

Perez-Invernon, F.J., Gordillo-Vazquez, F.J., Passas-Varo, M., et al. 2022. Multispectral optical diagnostics of lightning from space. Remote Sens., 14, 2057. doi:10.3390/rs14092057.

Peterson, M., Light, T.E.L., Mach, D. 2022. The illumination of thunderclouds by lightning: 2. The effect of GLM instrument threshold on detection and clustering. Earth Space Sci., 9, 2021EA001943. doi:10.1029/2021EA001943.

Peterson, M., Light, T.E.L., Mach, D. 2022. The illumination of thunderclouds by lightning: 1. The extent and altitude of optical lightning sources. J. Geophys. Res. Atmos., 127, e2021JD035579. doi:10.1029/2021JD035579.

Peterson, M., Light, T.E.L., Mach, D. 2022. The illumination of thunderclouds by lightning: 3. Retrieving optical source altitude. Earth Space Sci., 9, e2021EA001944. doi:10.1029/2021EA001944.

Peterson, M., Mach, D. 2022. The illumination of thunderclouds by lightning: 4. Volumetric thunderstorm imagery. Earth Space Sci., 9, e2021EA001945. doi:10.1029/2021EA001945.

Pizzuti, A., Bennett, A.J., Soula, S., et al. 2022. On the relationship between lightning superbolts and TLEs in Northern Europe. Atmos. Res., 270. doi:10.1016/j.atmosres.2022.106047.

Prácser, E., Bozóki, T. 2022. On the reliability of the inversion aimed to reconstruct global lightning activity based on Schumann resonance measurements. J. Atmos. Sol.-Terr. Phy., 235. doi:10.1016/j.jastp.2022.105892.

Pu, Y., Liu, N., Cummer, S.A. 2022. Quantification of electric fields in fast breakdown during lightning initiation from VHF-UHF power spectra. Geophys. Res. Lett., 49, e2021GL097374. doi:10.1029/2021GL097374.

Rabbani, K.M.G.R., Islam, M.J., Fierro, A.O., et al. 2022. Lightning forecasting in Bangladesh based on the lightning potential index and the electric potential. Atmos. Res., 267, 105973. doi:10.1016/j.atmosres.2021.105973.

Shi, D., Gao, P., Wu, T., et al. 2022. Pulse parameters and peak currents of return strokes observed by the Ningxia FALMA in the Chinese inland areas. Remote Sens., 14, 1838. doi:10.3390/rs14081838.

Silva, S.J., Keller, C.A., Hardin, J. 2022. Using an explainable machine learning approach to characterize earth system model errors: Application of SHAP analysis to modeling lightning flash occurrence. J. Adv. Model. Earth Sy., 14, e2021MS002881. doi:10.1029/2021MS002881.

Srivastava, A., Liu, D., Xu, C., et al. 2022. Lightning nowcasting with an algorithm of thunderstorm tracking based on lightning location data over the Beijing area. Adv. Atmos. Sci., 39(1), 178-188.

Stolzenburg, M., Marshall, T.C., Bandara, S., et al. 2022. Luminosity with large amplitude pulses after the initial breakdown stage in

intracloud lightning flashes. Atmos. Res., 267, 105982. doi:10.1016/j.atmosres.2021.105982.

Stough, S.M., Carey, L.D., Schultz, C.J., et al. 2022. Supercell thunderstorm charge structure variability and influences on spatial lightning flash relationships with the updraft. Mon. Wea. Rev., 150, 843-861.

Stracqualursi, E., Araneo, R., Faria, J.B., et al. 2022. Application of the transfer matrix approach to direct lightning studies of overhead power lines with underbuilt shield wires. Part I: Theory. IEEE T. Power Deliver., 37, 1226-1233.

Su, Z., Yang, J., Han, C., et al. 2022. Lightning transients of the overhead catenary system pillar and its adjacent grounding systems in a high-speed railway depot. IEEE T. Electromagn C., doi:10.1109/TEMC.2022.3144496.

Sun, H., Wang, H., Yang, J., et al. 2022. Improving forecast of severe oceanic mesoscale convective systems using FY-4A lightning data assimilation with WRF-FDDA. Remote Sens., 14, 1965. doi:10.3390/rs14091965.

Szabóné, A., Bozóki, K., Bór, T., et al. 2021. Automatic display of ELF measurements recorded in the Széchenyi István Geophysical Observatory. Geophysical Observatory Reports 2020, 35-40. doi:10.55855/gor2020.5.

Uhlirova, I.B., Popova, J., Sokol, Z. 2022. Lightning potential index and its spatial and temporal characteristics in COSMO NWP model. Atmos. Res., 268, 106025. doi:10.1016/j.atmosres.2022.106025.

Urbani, M., Montanya, J., van der Velde, O.A., et al. 2022. Multi-stroke positive cloud-to-ground lightning sharing the same channel observed with a VHF broadband interferometer. Geophys. Res. Lett., 49, e2021GL097272. doi:10.1029/2021GL097272.

Wada, Y., Morimoto, T., Nakamura, Y., et al. 2022. Characteristics of low-frequency pulses associated with downward terrestrial Gamma-ray flashes. Geophys. Res. Lett., 49, e2021GL097348. doi:10.1029/2021GL097348.

Wang, F., Zhang, Y., Deng, X., et al. 2022. Characteristics of regions with high-density initiation of flashes in mesoscale convective systems. Remote Sens., 14, 1193. doi:10.3390/rs14051193.

Wang, W., Zhu, B. 2022. Characterizing pulse attenuation of intra-cloud and cloud-to-ground lightning with E-field signal measured at multiple stations. Remote Sens., 14, 1672. doi:10.3390/rs14071672.

Wang, Y., Liu, K., Jia, J., et al. 2022. Investigation on the influence of balun to the lightning electromagnetic coupling effects of planar dipole working at 890-954 MHz. IEEE T. Electromagn C., 64(2), 464-471.

Wu, B., Lyu, W., Qi, Q., et al. 2022. High-speed video observations of needles in a positive cloud-to-ground lightning flash. Geophys.

Res. Lett., 49, e2021GL096546. doi:10.1029/2021GL096546.

Xu, L., Chen, S., Yao, W. 2022. Evaluation of lightning prediction by an electrification and discharge model in long-term forecasting experiments. Advances in Meteorology, 2022, 4583030. doi:10.1155/2022/4583030.

Xu, M., Qie, X., Pang, W., et al. 2022. Lightning climatology across the Chinese continent from 2010 to 2020. Atmos. Res., 275, 106251. doi:10.1016/j.atmosres.2022.106251.

Zhang, Y., Zhang, Y., Zou, M., et al. 2022. Advances in lightning monitoring and location technology research in China. Remote Sens., 14, 1293. doi:10.3390/rs14051293.

Zheng D, Zhang Y. 2021. New insights into the correlation between lightning flash rate and size in thunderstorms. Geophys. Res. Lett., 48, e2021GL096085. doi:10.1029/2021GL096085.

Zhu, Y., Stock, M., Lapierre, J., et al. 2022. Upgrades of the Earth Networks Total Lightning Network in 2021. Remote Sens., 14, 2209. doi:10.3390/rs14092209.

Atmospheric Electricity

https://www.iamas.org/icae/

NEWSLETTER

Vol.33 NO.1 May 2022

Edited by: Wenjuan Zhang (CAMS) and Haiyang Gao (NUIST)

REMINDER

Newsletter on Atmospheric Electricity presents twice a year (May and November) to the members of our community with the following information:

announcements concerning people from atmospheric electricity community, especially awards, new books...,

announcements about conferences, meetings, symposia, workshops in our field of interest,

brief synthetic reports about the research activities conducted by the various organizations working in atmospheric electricity throughout the world, and presented by the groups where this research is performed, and

a list of recent publications. In this last item will be listed the references of the papers published in our field of interest during the past six months by the research groups, or to be published very soon, that wish to release this information, but we do not include the contributions in the proceedings of the Conferences.

No publication of scientific paper is done in this Newsletter. We urge all the groups interested to submit a short text (one page maximum with photos eventually) on their research, their results or their projects, along with a list of references of their papers published during the past six months. This list will appear in the last item. Any information about meetings, conferences or others which we would not be aware of will be welcome.

Call for contributions to the newsletter

All issues of this newsletter are open for general contributions. If you would like to contribute any science highlight or workshop report, please contact Weitao Lyu (wtlu@ustc.edu) preferably by e-mail as an attached word document.

The deadline for **2022 fall issue** of the newsletter is **Nov 15, 2022**.

PRESIDENT

Xiushu Qie

Chinese Academy of Sciences

E-mail: qiex@mail.iap.ac.cn

SECRETARY

Weitao Lyu

Chinese Academy of Meteorological Sciences

E-mail: wtlu@ustc.edu